Behavioral and Neurophysiological Effects of Electrical Stunning on Zebrafish Larvae

David-Samuel Burkhardt
University of Tübingen
Claire Leyden
University of Tübingen
Carina Thomas
University of Tübingen
Christian Brysch
University of Tübingen
Florian Alexander Dehmelt
University of Tübingen
Aristides B. Arrenberg
aristides.arrenberg@uni-tuebingen.de

University of Tübingen https://orcid.org/0000-0001-8262-7381

Article

Keywords: zebrafish, animal welfare, 3R, refinement, electrical stunning, electric fields, euthanasia, death, killing, calcium imaging, righting response, heartbeat, vision, calcium wave, slowly spreading depolarization

Posted Date: March 28th, 2024

DOI: https://doi.org/10.21203/rs.3.rs-4021167/v1

Additional Declarations: There is **NO** Competing Interest.

Abstract

In today's scientific research, two methods dominate the way zebrafish larvae are euthanized after experimental procedures: anesthetic overdose and rapid cooling. Although easy to apply, the anesthetic MS-222 takes about a minute to act, fish show aversive reactions, and inter-individual differences limit its reliability. Rapid cooling only kills larvae after many minutes and is not listed as approved method in the relevant EU directive. Electrical stunning is a promising alternative euthanasia method but hasn't been established yet for zebrafish. In this study, we characterize both behavioral and neurophysiological effects of electrical stunning in 4 dpf zebrafish larvae. We identified the electric field magnitude and stimulus duration (32 s at 50 V/cm) that reliably euthanize free-swimming larvae and agarose-embedded larvae and provide an easy-to-implement protocol. Behavioral analysis and calcium neurophysiology show that larvae lose consciousness very fast and stop responding to touch and visual stimuli (< 1 second). Electrically stunned larvae do not show coordinated brain activity anymore and their brains will instead undergo a series of concerted whole-brain calcium waves over the course of many minutes before the ultimate cessation of all brain signals. Consistent with the imperative of implementing the 3R at all stages of animal experiments, the rapid and reliable euthanasia achieved by electrical stunning has the potential to bring about a real refinement of the welfare of more than 5 million zebrafish used annually in biomedical research worldwide.

Introduction

The zebrafish (*Danio rerio*) is one of the most common model organisms in neuroscience and biomedical research, with more than 5 million individuals used in animal experiments annually [1,2]. Because this figure excludes many animals used in breeding instead of experiments, or animals used below the legal age limit (5 days post fertilization, or dpf), the total number is even higher. Also, it is expected that the overall number will further rise due to the promising characteristics of this model organism and its continued spread into many areas of research [3]. Good scientific practice alone already requires well-designed and planned animal experiments [4], but this is further reinforced by an increasing awareness of the use of animals for scientific research in society [5] and the still unanswered question whether and in which form fish perceive and suffer from pain [6,7 8]. Within the EU, directive 2010/63/EU specifically enumerates the legal euthanasia methods for laboratory fish: percussive blow to head, anesthetic overdose and electrical stunning. However, uncertainties persist concerning the application of these methods to zebrafish larvae (Fig. 1A).

First, percussive blows to the head are not practical or safe to perform because larvae are only 4 mm in size [9]. Second, overdose of the anesthetic MS-222, which in adult fish leads to death through asphyxiation and hypoxemia due to blocked gill ventilation, does not reliably work on zebrafish larvae, as they rely on cutaneous gas exchange during early gill development [10]. Only at 12–14 dpf cutaneous gas exchange is no longer sufficient to meet the minimal respiratory requirements [11]. Thus, despite the onset of cardiac arrest and a high concentration of MS-222 (900 mg/l), zebrafish larvae regain consciousness

when transferred back to normal fish water [10]. Moreover, MS-222 triggers aversive reactions in zebrafish, as they can smell the anesthetic even before the onset of the anesthetic effect [12]. Thus, behaviors such as piping, twitching, and erratic swimming have been observed in both unbuffered and buffered solutions [13]. They even prefer to spend significantly more time in a dark environment than in a bright environment containing the anesthetic MS-222 which may indicate that fish would rather undergo discomfort than being exposed to MS-222 [14]. Furthermore, the efficacy of MS-222 is variable across animals [11].

Another euthanasia method that is not universally permitted by law for zebrafish but is often used after special approval by the local authorities, is rapid cooling, in which the animals are placed in ice water. The resulting hypothermic shock is thought to cause death by slowing the rate of cellular activities and neural impulses, finally leading to cardiac arrest [10] and it is mostly considered a humane alternative to the use of an anesthetic, not least because fish exhibit signs of distress over a much shorter period than MS-222-treated animals [13,15]. While the onset of unconsciousness is likely fast, zebrafish larvae easily survive long periods in ice water and must be kept in a freezer overnight to ensure mortality; rapid cooling in larvae younger than 14 dpf in fact requires as long as 12h minimal exposure to cold for reliable euthanasia [16]. This highlights how little is known about the exact time death results from this method, and prolongs the time window in which suffering is possible, if e.g. the hypothermic larvae briefly warm up to 11° before being placed in the freezer[17].

Legislation including the relevant EU directive alternatively permits the application of electricity for euthanasia and refers to this as “electrical stunning”, even if death, not stunning, is the intended outcome While electrical stunning protocol have successfully been established for larger fish [18], its suitability has scarcely been investigated for laboratory zebrafish[19] and electrical stunning has therefore never been successfully established as a humane euthanasia method for zebrafish. Knowledge about reliable parameters including voltage gradient, exposure duration, voltage type, the needed water conductivity and the resulting power density in the fish body are missing [1]. There is also no known adequate and approved equipment that could be used for this purpose [15]. Euthanasia by electrical stunning is most likely to be achieved by either asphyxiation of the stunned fish or by cell death due to unrecoverable damage to the cell membrane integrity of the fish. Larger cells seem particularly susceptible to electric field-induced membrane damage[20], which is why the effectiveness of electrical stunning is expected to increase with fish size. Also, different voltage types (such as direct current, DC; pulsed direct current, PDC; or alternating current, AC, and the associated frequencies) are thought to directly influence mortality rate and tissue damage [21–25]. Different aspects of electrical stunning have been investigated for various fish species at different stages of development, but the parameters were often not systematically varied and the effects of electrical stunning on zebrafish behavior and brain activity were not systematically recorded (e.g. [19,21,26]). To the best of our knowledge, there is not a single study where potential suffering and stress associated with electrical stunning was quantified in zebrafish, nor where neural correlates of such experiences were quantified, such as changes to sensory processing induced by the euthanasia method.

Here, for the first time, we investigated electrical stunning as an alternative humane euthanasia method for zebrafish larvae both on the behavioral and neurophysiological level using calcium imaging (Fig. 1B and C). We examined and compared different voltage types (DC, PDC, AC) and exposure durations (2 s to 32 s) and their influence on mortality rate and tissue damage. We identify a set of parameters which reliably work at a voltage frequency close to the mains frequency of 50/60 Hz and for a standard embryo medium conductivity of 670 µS/cm [27], resulting in a 100% mortality rate. Besides behavioral examination we also investigated neuronal activity patterns using calcium imaging, confirming the total loss of coordinated and stimulus-associated neuronal activity and behavior during and after electrical stunning.

Results

Mortality rates and behavioral effects of electrical stunning

To identify the optimal parameter set encompassing voltage gradient, voltage type, and exposure duration for electrical stunning, we exposed larvae to DC, AC (60Hz), or PDC (60Hz or 6Hz, duty cycle = 50%) electric fields (50 V/cm) in the water bath (Fig. 1, n = 20 larvae per condition). Mortality was assessed as loss of equilibrium, lack of locomotor activity, lack of gill ventilation, and lack of responses to tactile stimuli (Fig. 2C, Methods). For five different exposure durations (from 32 s to 2 s in logarithmic steps), we conducted four independent trials involving five larvae each. At 32 s exposure, all voltage types resulted in 100% mortality. For 16 s exposure, only 60 Hz PDC was not able to reach a 100% mortality rate. At 8 s exposure, significant divergence in mortality rates among voltage types emerged for the first time (z-test for proportions, $p < 0.01$), with rates dropping below 20% for all types at 2 s (Fig. 2D). Behavioral loss of equilibrium was immediate across all voltage types, occurring within 900 ms (AC: 0.89 s ± 0.38 s, DC: 0.64 s ± 0.25 s, PDC 60 Hz: 0.73 s ± 0.28 s, PDC 6 Hz: 0.72 s ± 0.22 s (± STD)), indicating an instant onset of anesthesia (Fig. 2E) [28].

Depending on the voltage type used, several morphological changes including body curvature, opaque brain tissue and sometimes fractures could be observed for longer exposure durations (32 s and 16 s) for all voltage types. Morphological abnormalities were recorded directly, 15 minutes and 30 minutes after exposure. These included visible destruction of tissue, skin and eyes as well as severe deformation of the body axis (lordosis, kyphosis, and scoliosis) for DC, small to medium body axis deformation for AC, and medium tissue destruction and body axis deformation for PDC (Fig. 2H and supplementary Fig. 2). None of the larvae exhibiting abnormalities survived.

Since AC voltage and exposure durations of 16 and 32 s achieved 100% mortality with a fast onset and only minimal morphological abnormalities, we next refined these parameters with regard to the voltage gradient. We tested five different voltage gradients (from 45 V/cm to 20 V/cm) for 16 s and 32 s exposure duration. Already for 45 V/cm, mortality rates differed significantly and only the 32 s trial still reached 100% mortality rate (z-test for proportions, $p < 0.0001$) (Fig. 2F). We therefore concluded that AC (60 Hz), 50 V/cm and 32 s is a reliable and effective parameter set to achieve 100% mortality rate and it was used

for all subsequent calcium imaging experiments to assess the effects of electrical stunning on the neurophysiological level.

Electrolysis and Joule heating

During experiments using the exposure chamber, electrolysis could be observed as small bubbles formed at the electrode surfaces. Because the basicity of the E3 medium remained stable at pH 7, this was not investigated further. However, electrolysis effects should be explored more comprehensively for a final implementation of electrical stunning.

Furthermore, an increase in temperature and thus in electrical current was observed during exposure to AC, DC and PDC for all exposure durations. Temperature increases ranged from 1.26 ± 0.33°C for PDC (60 Hz) and 2 s exposure duration to 24.25 ± 0.22°C (± STD) for DC and 32 s exposure duration (supplementary Fig. 3). The temperature rise was 13.3 ± 0.53°C for AC (60 Hz), 50 V/cm, 32s; with 36.1°C being the maximum temperature reached. The observed change in temperature is due to Joule heating, where an electric current heats a medium. In turn, the conductivity changes which again influences the current magnitude. These effects led to a rise in power density in the exposure chamber, which in principle could have influenced the mortality rates (Fig. 2G). No rise in temperature was observed during calcium imaging experiments (see below), where a single larva was agarose-embedded between two small electrodes. This is most likely due to the significantly smaller electrode surfaces and the proportionally larger E3 volume in the Petri dish, which serves as a heat sink. To rule out that the temperature rise and increased power density affect mortality rates for AC at 50 V/cm and 32 s exposure duration, and to thus ensure comparability between the mortality rate experiments using the exposure chamber and the calcium imaging experiments not using it, a transfer experiment was carried out where single agarose-embedded larvae were exposed to an AC field with 50 V/cm for 32 s using the small electrodes (see Methods). After exposure, larvae were freed from agarose and mortality was determined using the same behavioral criteria as used for free-swimming experiments. No difference in mortality rate was observed (N = 6 larvae with 100% mortality rate). Thus, even in the absence of a rise in power density associated with the exposure chamber, 100% mortality can be achieved with AC at 50 V/cm and a 32 s exposure duration.

Swim bursts during electrical stunning

Within the first seconds of exposure to any tested electrical field, we observed short bursts of tail movements, either during or after loss of equilibrium (supplementary Video 1). If this corresponded to a planned locomotion behavior, that might have implications regarding the state of the animal and associated potential of suffering. To rule out any such kind of active locomotion, we recorded a high-speed video of a single embedded larva with its tail cut free and exposed to an AC field at 50 V/cm for 32 s (Fig. 3A). A kymograph of the total angle of the tail revealed a strong initial tail deflection at exposure onset followed by a tail beat frequency perfectly matching the 60 Hz sinusoidal frequency of the electric field applied, strongly suggesting that the observed muscle movements were passively driven by the electric field (Fig. 3B, Fig. 3D, supplementary Video 2). Furthermore, both tail beat amplitude and standard

length[29] decreased during exposure (pre-exposure: 3.9 mm, intra-exposure: 3.1 mm, Fig. 3E), presumably as a result of bilateral tail muscle contraction driven by the electric field. Also, the spatio-temporal curvature pattern of the tail differed drastically for tail undulations during exposure as compared to pre-exposure (Fig. 3C). During the spontaneous swim bout, the point of maximal curvature travels along the tail in rostro-caudal direction for each tail undulation, which is conducive for forward swimming.[30] However, during electric field exposure the stereotypic spatiotemporal pattern could not be observed, i.e. the complete tail contracted at once in abnormal, bilaterally synchronized fashion.

The observed phenomenon might be related to the "pseudo-forced swimming" described before [31], although the voltage type used in that study was DC.

Loss of visually driven neural activity during electrical stunning

To quantify and compare neuronal activity before, during and after electrical stunning, two-photon calcium imaging was performed while applying a simple and strong visual ON-OFF stimulus (full-field flash) and simultaneously exposing larvae to an electric field (AC, SIN, 60 Hz, 50 V/cm, 32 s). Recordings were done in the optic tectum, which is known to be a hub in visual processing and contains different populations of neurons well responding to ON and OFF flashes [32,33]. Because the visual system of zebrafish larvae develops rapidly, strong optokinetic responses and associated sensory driven neural activity are already established by 4 dpf [34,35]. The absence of such sensory driven activity can thus serve as a reliable indicator of defective neural processing.

Mean fluorescence time courses across all pixels obtained from the calcium recordings before (baseline), during (shock) and after (recovery) electrical stunning revealed drastic changes in activity patterns and overall intensities (Fig. 4B). Exposure to the electrical field also gave rise to a fast-propagating calcium wave (< 2 s) with high mean fluorescence intensities along with strong spatial drifts (> 20 µm), resulting in permanent morphological changes that impeded consistent segmentation of individual neurons across recording time (supplementary Video 3). After exposure, mean fluorescence intensity across each image frame decreased until the occurrence of further, slowly (> 2 s) propagating calcium waves, with different characteristics than the initial wave (Fig. 4B). Due to these strong changes in fluorescence intensity, adjustment of laser power and PMT gain between individual recordings were necessary to avoid overexposure and damage to the PMTs. Thus, absolute fluorescence intensities cannot and should not be compared across recordings.

To investigate whether visual processing still occurred during and after electrical stunning, the mean power spectral density (PSD) of all pixels within a recording was analyzed across all fish, where for intact vision-related processing the stimulus main frequency (0.1667 Hz) should not be significantly affected by spatial drifts of the larva in the recording window (supplementary Fig. 4). As expected, PSD analysis revealed a total loss of the visual stimulus main frequency (0.1667 Hz) during shock and recovery ($p < 0.01$ between 0 and 0.22 Hz for shock and recovery recording, two-way repeated measure ANOVA followed by Tukey's HSD test, Fig. 4C-D). A further PSD analysis only covering the period during exposure

to the electric field (32 s) confirmed this observation (Fig. 4D, middle, inset). Furthermore, the mean power density strongly increased towards lower frequencies during shock and recovery recordings, representing the observation of brain-wide, slowly changing calcium intensity.

Next, we segmented neurons in each the baseline and recovery recording to ask how the population tuning to the visual stimuli changed. The optic tectum contains diverse sets of neurons, some correlated and other anti-correlated or not correlated with our luminance stimulus. Also, on average, fluorescence time courses of neurons should inherit some form of periodicity as the stimulus itself consisted of various periodic parts. In contrast, during and after exposure all these characteristics should have vanished to confirm loss of intact neural processing and the effectiveness of electrical stunning as a euthanasia method. In total, 4958 segmented ROIs (regions of interest) were analyzed during baseline recording and 3369 ROIs during recovery (n = 7 fish). The difference in number of detected ROIs is due to the technical difficulty of detecting ROIs during recovery. Neurons in the optic tectum showed diverse activity patterns during baseline recording with regard to visual stimulation, where 3.5% of the overall number of neurons were correlated or anti-correlated to the visual regressor with a correlation coefficient above 0.3 (Fig. 4E and Fig. 4H). During recovery recordings, not a single neuron had a correlation coefficient higher than 0.3. Also, a Levene-test revealed a significant difference in the variance of correlation with the visual regressor between both recordings ($p < 0.0001$). To characterize the stimulus-related activity, we quantified the pairwise cross-correlation between the 20% best correlated neurons within each fish for both baseline and recovery recording (Fig. 4F). Neurons within each matrix were sorted by their correlation coefficient from positive to negative, resulting in a structure with two visible anti-correlated populations (red and blue) during baseline recording. These populations correspond to neurons responding to either the ON- or OFF-phase of the visual stimulus. No similar structure could be found during the recovery recording, where almost all neurons correlated with each other, which could be explained by an overall synchronous decrease in fluorescence due to the fading out of the initial calcium wave. Finally, an autocorrelation function (ACF) of both recordings yielded a perfect periodic pattern for the baseline recording representing the periodic stimulus-related activity pattern, and nothing but linear decrease during the recovery recording (Fig. 4G).

All these results strongly indicate that during electrical stunning and afterward, no neural processing with respect to visual perception was possible, as the dominance of monotonous calcium signals indicates non-intact brain activity and presumable loss of sensation.

Discussion

In this study we investigated electrical stunning as an alternative euthanasia method for zebrafish larvae. We systematically evaluated different voltage types, voltage gradients and exposure durations, resulting in a robust parameter set that can be implemented under real-world conditions. We further demonstrated that observed tail movements during exposure are unrelated to any kind of volitional locomotion and that electrical stunning provokes an immediate loss of coordinated neuronal activity – and therefore, likely suppresses any sensation that could arouse suffering. Crucially, larvae never recovered from this terminal

state, and their rapid loss of equilibrium confirms that electrical stunning minimizes the remaining time window before complete incapacitation, especially compared to previously established euthanasia methods.

Reliable parameters are straightforward to implement

One of our major aims was to not only comprehensively examine the effects of electrical stunning on behavioral and neurophysiological level, but to also devise a reliable parameter set that can be implemented in practice across international and disciplinary boundaries. An important consideration therefore was to also examine a sinusoidal AC voltage with a frequency near 50 or 60 Hz, as it is common in many countries. While both 32 s and 16 s exposures lead to 100% mortality at 50 V/cm (Fig. 2D), we recommend the longer of the two to account for possible variations in specific future implementations; this also appears prudent considering that, while we confirmed the loss of stimulus-associated neural activity for a 32 s exposure, we did not repeat these experiments under 16 s exposure. Despite Joule heating raising the resulting power density to 1.4 W/cm^3 after 32 s during behavioral assays (Fig. 2G), the calcium imaging experiments showed that 0.85 W/cm^3 are in fact sufficient to reliably euthanize zebrafish larvae. This is in accordance with published findings that there is no influence on survival rate for a power density of 0.00086 W/cm^3 using AC at 12.5 V/cm and 2000 µS/cm [36] and successful euthanasia of zebrafish larvae with a calculated power density of 0.7 W/cm^3 with PDC at 50 Hz, 25 V/cm and 1120–1130 µS/cm [19]. Although the conductivity of small fish species is thought to be less than 30 µS/cm [37] and therefore the conductivity of a zebrafish larva is most likely even smaller, our medium for electrical stunning with a conductivity of 680 µS/cm was chosen specifically to be consistent with a standard E3 embryo medium (5 mM NaCl, 0.17 mM KCl, 0.33 mM $CaCl_2$, 0.33 mM $MgSO_4$ and 10^{-5}% Methylene Blue) as it is commonly used for zebrafish larvae [27].

The suggested parameters should be easy to implement in an electrical stunning setup due to their characteristics and the principle layout of the exposure chamber introduced in our experimental setup (Fig. 1B and supplementary Fig. 5) might provide a possibility to build and establish safe and adequate devices as required by the EU directive 2010/63/EU [15].

Electrical stunning reduces time window to onset of euthanasia

We have demonstrated that loss of equilibrium can be reliably induced within a single second using electrical stunning, which is an important aspect when evaluating an euthanasia method [38]. On a behavioral level, an animal is likely to be unconscious from the timepoint on its loosing it's righting reflex (which in our study is equivalent to the loss of equilibrium) [28]. Tricaine (MS-222) is known to work relatively slowly in this respect, as it takes between 25 and 34 seconds for adult zebrafish to loose equilibrium at a concentration of 250 mg/l [13,39,40]. Even at 336 mg/l it takes about 15 s for larvae until the loss of the righting reflex [17]. Though, for rapid cooling (2–4°C) the time window to onset decreases to 5–9 s for adult zebrafish [13,40]. The much faster onset time for electrical stunning therefore has an

immediate effect on the reduction of any possible stress and suffer. Aversive reactions shown by larvae as reported for Tricaine usage [12–14] could not be observed.

AC is the best suited voltage type for electrical stunning

Depending on voltage type and voltage gradient, different injuries like tissue disruption, vertebral dislocations and even fractures are known to occur in fish. These injuries most likely arise from strong muscle contractions caused by either direct electrical stimulation of muscles or of the neuromuscular pathway and are influenced by the voltage type used, as well as the voltage gradient and frequency [18,41,42]. There are different findings regarding how different voltage types effect mortality and injuries. According to Reynolds, J.B. (1996), using DC or reducing the frequency at PDC results in less injury to fish whereas AC is most likely to cause tetany, potentially resulting in injury and mortality [25]. Also, Snyder (2003) reported that spinal injuries have mostly been associated with AC [43] and there are numerous reports about non-DC waveform which together with different frequencies negatively affected injury and survival rates [18,42–45]. However, this does not seem to be the case regarding embryos and zebrafish larvae which are found to be more vulnerable to DC [21,22,36,46]. This concurs with our findings, where DC (50 V/cm, 32 s) lead to severe tissue destruction and ruptures (Fig. 2H). DC treatment was also associated with the highest reached temperatures due to Joule heating (up to 46.9 ± 0.4°C), which likely contributed to the morphological defects of larvae via thermal denaturation of proteins. During treatments with AC, on the other hand, the temperature only increased mildly and stayed below 38°C (50 V/cm, 32s, AC: 35.03 ± 0.77°C), a temperature which is frequently used for live zebrafish in genetic experiments [47–50]. While the DC-associated injuries and body deformations are unlikely to significantly impact larval welfare relative to AC, given DC's loss of equilibrium also occurring in within 1 s (0.64 s ± 0.25 s), they might misconstrue electrical stunning as an unsuitable euthanasia method. In avoidance of that and taking into account that a good euthanasia method should also consider the emotional effect on observers and operators [38], we endorse AC as the most compelling voltage type for electrical stunning applications on zebrafish larvae.

Electrical stunning with AC is followed by wide-spread propagating calcium waves

Over the course of investigating neuronal activity during and after electrical stunning, we observed a strong synchronous rise of intracellular calcium (also referred to as a fast-propagating calcium wave) alongside the onset of the electrical field as well as concomitant morphological changes. Most likely, this first wave was caused by the influx of calcium from extracellular space driven by the electric field [51]. This influx might in turn have led to ATP depletion and mitochondrial failure due to the loss of membrane potential, further causing imbalance of calcium and potassium, and finally cell death [52–55]. The exact mechanism underlying cell and organismal death in zebrafish larvae via AC-based electrical stunning still remains unclear, but previous research provides indications about different pathways of cell death following exposure to electrical fields [56]. Although we did not characterize the differences between the initial fast-propagating and following slow-propagating calcium waves in detail, they seemed to differ in

propagating speed, maximum calcium intensity and place of origin. The latter ones (as seen by eye) might be similar to earlier observations in zebrafish larvae, where a slow wave occurred after cardiac arrest, traveling in a caudal-rostral direction and thought to be associated with neuronal death and brain damage [57]. Other brain-wide calcium waves in zebrafish larvae, akin to what is called a spreading depolarization [58,59] could be observed in the context of heat-induced neural dysfunctions [60]. In rats, the presence of a large-amplitude EEG-wave after decapitation has been described. It was assumed, that the wave reflects a massive opening of ion channels (depolarizing wave), which occurred due to neurons lacking energy which might have led to a breakdown of transmembrane potential, leading to oscillations and the observed wave [61,62]. Though a comprehensive elucidation of the mechanism and relevance of these slow-propagating calcium waves necessitates further investigation, our findings, alongside perception of visual stimuli and behavior of larvae during and after electrical stunning, argue against their association with suffering or stress.

Electrical stunning is an effective alternative euthanasia method

In summary, our results suggest that electrical stunning, when using the proposed parameter set, is an effective euthanasia method for zebrafish larvae. Besides immediate loss of equilibrium, the irrevocable loss of coordinated and sensory-driven neuronal activity strongly indicate rapid onset of unconsciousness during treatment [28]. As far as we know, the only other studies examining neuronal activity alongside exposure of electrical fields to fish were performed applying EEG on African catfish and cichlids, where during exposure a general epileptiform insult could be observed, which was followed by fibrillation after electrical stunning [63,64]. Our observed slowly propagating calcium waves after electrical stunning encourage further investigation, but they do most likely not influence the efficacy of the euthanasia method itself or the animal's welfare. Given the fact that electrical stunning is already a permitted euthanasia method for fish in the EU, its implementation in laboratory routines could plausibly contribute to a refinement in the sense of 3R[4,65] across many disparate research labs.

Materials and Methods

Animals

Animal experiments were permitted by the local government authorities (Regierungspräsidium Tübingen) and conducted in accordance with German federal law and Baden-Württemberg state law. Zebrafish larvae (*Danio rerio*) were reared on a 14/10 h light/dark cycle at 28°C in E3 medium (5 mM NaCl, 0.17 mM KCl, 0.33 CaCl, 0.33 MgSO4) with 0.01% methylene blue. Wildtype (*nacre* +/-) larvae were used for the mortality rate and behavioral experiments. Transgenic zebrafish expressing GCaMP6f [*Tg(HuC:H2B-GCaMP6f)jf7Tg*] were used for the two-photon calcium imaging experiments. The top 10–20% of larval zebrafish with high calcium indicator expression levels were selected from all fish at 3 dpf for in vivo calcium imaging experiments. All behavioral and calcium imaging experiments were performed on 4 dpf zebrafish larvae at room temperature. Supplementary Table 1 contains a list of experimental groups and animals used per group.

Exposure chamber for mortality rate experiments

To determine mortality rates of multiple free-swimming larvae, an exposure chamber covering a volume of 50x36x15 mm was designed and build out of polystyrene. The internal dimensions of the exposure chamber represent a trade-off between the space needed to safely exposure multiple larvae to an electric field, and the required voltage gradients. To protect against leakage currents, the programmable power source was connected to the exposure chamber by a residual-current circuit breaker (F200, B Type, ABB Ltd (Asea Brown Boveri), Zürich, Switzerland). This guaranteed safe operation for both AC and DC voltages. Two stainless steel electrodes (36x15 mm) with a thickness of 1 mm were placed inside the chamber at a distance of 50 mm. A custom-made 3D-printed electrode holder was used to hold the electrodes in place and to ensure the exact distance of 50 mm. This electrode holder also included a rigid net with an aperture of no more than 405 µm (PA-405/47, Eckert, Waldkirch, Germany), in which larvae could be placed during exposure. This ensured that larvae were always exposed to the center of the electric field (supplementary Fig. 5 and supplementary Fig. 7A). Electrodes were constructed by the precision mechanics workshop of Eberhard Karls University, Tuebingen, Germany. All polymer components were constructed and 3D-printed in the lab (Ultimaker3, Ultimaker B.V., Utrecht, Netherlands, ink: Ultimaker Material PLA Black, diameter 2.85 mm). For safety reasons, operation of the exposure chamber depends on a snap-action switch which require a closed lid. The lid and bottom of the chamber are transparent to enable diffuse back illumination at 920 nm from below and behavioral recording from above. An LED array containing 48 LEDs with a 50° emission angle and a diffuser (frosted glass) was used for illumination. Recording was done at up to 30 Hz using a camera (DMK23UV024, The Imaging Source Europe GmbH, Bremen, Germany) with a 6 mm objective and an IR longpass filter (SCHOTT RG780, Edmund Optics Inc., Barrington, USA). Both the power source and the camera recording were controlled by the custom written Python software “synchASR2000-control”. The software allowed to individually set voltage type (DC, PDC, AC), overall voltage, maximum current, frequency and the exposure duration.

Determining mortality rates

For each experiment, the exposure chamber was filled with 24 ml of room-temperature E3 medium (680 µS/cm conductivity). Five larvae were transferred into the chamber, followed by a 5 min acclimatization period. After that period, the temperature of the E3 medium inside the chamber was measured once using a digital thermometer (GMH 3200 Series, GREISINGER, Regenstauf, Germany) and the lid was closed. An electric field was then applied for a specific exposure duration. In case of controls, no electric field was applied. During the exposure, larvae were video-recorded. The recording was synchronized with the onset of the electric field via the Python software using a timestamp. Immediately after the exposure, the lid was opened, and temperature was measured again. Larvae were then moved into a dish of fresh E3 (room temperature). To determine mortality rates, all larvae were visually examined via a stereo microscope directly after exposure to an electrical field and a second time after a 30 min recovery period in fresh E3 (Fig. 2B). Mortality was defined by the following criteria: no activity of any kind, loss of equilibrium, no operculum movement, and no startle response (tested by a strong tactile stimulus).

Together with muscle tone and cardiac failure (which were not assessed here), these criteria correspond to the fourth stage of anesthesia in fish, describing overdose [66]. Muscle tone observation was excluded due to the ability of electrical fields to cause muscle tension. Cardiac arrest on the other hand is not a suitable criterion for death in larval zebrafish, because their small size ensures that oxygen diffusion into vital tissue is sufficient for survival even after the heart stops beating [10]. Heartbeat may persist for up to 10 min after euthanasia with MS-222 and 40 min after hypothermic shock [10]. Some studies even report that MS-222 treated larvae were able to recover their heartbeat when subsequently transferred to fresh water [10,11]. Also, in our study, cardiac arrest rates differed from mortality rates for exposure durations between 2 and 32 s (supplementary Fig. 8). Larvae were only considered dead, if all tested criteria were met at both of the two observation points (directly after exposure and after the 30 min recovery period) (Fig. 2C). After the second observation point, all larvae were put into ice water to ensure proper euthanasia for potentially survived fish. In total 600 fish were used in 30 different groups (supplementary Table 1). Significant differences between different voltage types and between exposure durations within each voltage type were determined by z-test for proportions followed by Bonferroni correction. A pilot trial with 20 larvae anesthetized with MS-222 (168 mg/l) and 20 non-anesthetized larvae exposed to 50 V/cm for 32 s revealed no increased mortality rates for MS-222 and all subsequent experiments were carried out without anesthetic (z-test for proportions, $p > 0.05$., supplementary Fig. 1).

Determining loss of equilibrium

Loss of equilibrium was determined by hand using the video recordings from the mortality rate experiments and the image processing package Fiji [67]. The time difference between the exposure onset of electrical stunning and the first frame where larvae departed from the upright position was measured. Not all recorded larvae could be analyzed, because they sometimes swam into the shadow cast by the electrode frame, which made it impossible to observe the time point of loss of equilibrium. Therefore, the number of larvae analyzed in this regard differed from the total number of larvae recorded. In total 295 fish were analyzed.

Swimming burst analysis

A high-speed recording (IDT iN8-S1 camera) with a sampling rate of 500 Hz was performed on a single agarose-embedded 4 dpf larva (nacre +/-) using the exposure chamber without the rigid net (Fig. 3A). Agarose was removed around the tail to observe exposure-related movements. Recording was performed for 10 seconds (exposure onset was approximately 1 second after the start of recording). Electrical stunning was performed with a sinusoidal AC field, 60 Hz, 50 V/cm, for 32 s.

To analyze the recordings, images were first smoothed using a median filter (filter size: 20x20 pixel) to remove noise. Afterwards, the gray values of all pixels were first inverted and then binarized. Areas smaller than 600 pixels in size were removed to clear the image, leaving only the silhouette of the fish. A skeleton of the silhouette representing the spine of the fish was computed to track tail deflections. Lateral displacement of the tail was defined as the distance (in pixels) of each skeleton pixel to the fish's original

rostro-caudal axis, normed to the mean displacement during spontaneous swim bout and field exposure. Total tail angle (in degrees) was calculated for each frame by computing the angles between all neighboring pixels on the skeleton and then taking the sum along the entire tail. Tail length was normalized to the shortest skeleton computed using 1D interpolation. In total, two fish were recorded and analyzed.

Setup for simultaneous calcium imaging and electrical stunning

For calcium imaging experiments, a two-photon IR laser (Coherent Chameleon Vision S, Coherent Inc., Santa Clara, USA) at a wavelength of 920 nm was used and calcium-signals were recorded using a movable-objective microscope (MOM; Sutter Instruments, Novato, USA) with GaAs photomultiplier tubes (PMT), C7319 Hamamatsu preamplifiers and the MScan software (2016 version) by Sutter. All recordings were conducted in the optic tectum, scanning a single plane per fish approximately 40–70 µm deep with a 20x/1.0 objective (Zeiss W Plan-Apochromat 421452-9800, Jena, Germany) at a frequency of 2 Hz and a magnification of 1.8x. To conduct calcium imaging alongside simultaneous visual stimulation and exposure to an electric field, a setup containing a LED ring with 18x 650 nm LEDs and a centered 50 mm Petri dish with two small stainless-steel electrodes was developed. The electrodes (2x3 mm, 0.5 mm thick) were placed at a distance of 3 mm in the Petri dish using a custom-made 3D-printed frame. The frame enclosed the electrodes from three sides to avoid any unwanted possible contact with the microscope objective (supplementary Figs. 6 and 7C). To connect the electrodes to the power source, a 200 µm thin copper plate was welded to their back sides to allow soldering of cables. The power source was controlled by the custom written Python software ”synchASR2000-control”. To present a strong visual ON/OFF-stimulus, the LED ring was connected to an Arduino NANO, controlling power supply of the LEDs. To gate the LEDs during laser scanning, the Arduino NANO considered the fly-back signal provided by the MOM. ON/OFF-signals from the LEDs, fly-back signal from the MOM and the onset-signal of the electrical field were recorded at 100Hz via an Arduino UNO and another custom-written Python software called “recSignals-control”. The whole setup was electrically separated from the microscope objective by a modified SM1L05 lens tube containing an insulating plastic spacer.

Calcium imaging alongside electrical stunning and visual stimulation

For each experiment, a single zebrafish larva was embedded in 1.6% agarose gel (Biozym Sieve GeneticPure Agarose 850080 mixed with E3 medium) between the electrodes (Fig. 4A). Agarose is electrically neutral, so the electrical conductivity of the gel is determined by the liquid added [68]. Therefore, it can be assumed that the conductivities of E3 medium and agarose gel were approximately the same and it was unlikely to affect the homogeneity of the electric field. Each experiment consisted of three subsequent recordings: baseline recording (6 min, of which 3 with visual stimulation), shock recording (6 min with visual stimulation) and recovery recording (12 min with visual stimulation) (Fig. 4B). Recordings were done in the optic tectum which is known to be a hub in visual processing and it contains different populations of neurons well responding to ON and OFF flashes [32,33]. In total 7 fish were imaged.

Analysis of ROIs and Cross-Correlation Matrices

All data analysis was done in Python. Baseline and recovery recordings were registered to standard deviation (STD) z projection and regions of interest (ROIs) were segmented using suite2p [69]. The calcium signal ($\Delta F/F_b$, i.e. fluorescence changes relative to baseline) at time point t was calculated as in Leyden et al. (2022) [17]. The calcium signal of each ROI was calculated for the second half of the baseline recording (visual stimulus present), and during the period preceding onset of a slow propagating wave for the recovery recording, which differed across trials. The overall number of ROIs for baseline and recovery recording differed, which could be explained a combination of morphological changes during electrical stunning, the overall decrease in calcium activity, as well as the increase of synchronized activity among ROIs which led to poor segmentation results in the recovery recordings.

Regression-based identification of stimulus-encoding neurons was used in this study to quantify alterations of vision-related activity during and after electrical stunning [70]. For this purpose, an ON-regressor was computed by first resampling the recorded ON/OFF-signals of the visual stimulus to 2 Hz and then convolving them with a calcium impulse response function (CIRF) using an exponential decay time constant of 1.61 s for GCaMP6f. ROIs were then correlated with the ON-regressor to test how well their activities matched the expected calcium signal of a neuron responding to light onsets. Distributions of correlation coefficients for baseline and recovery recording were analyzed via a Levene-test.

To generate cross-correlation matrices, ROIs were sorted by their correlation coefficient (from positive to negative correlation with the stimulus) and a cross-correlation matrix of the 20% best correlated ROIs was computed. Matrices of all fish were brought to the same size (mean size of all matrices) using linear interpolation. A weighted average matrix was then computed, based on the total number of ROIs per fish.

Power spectral density analysis

Welch's power spectral density (PSD) method was used for estimating the power density of fluorescence at different frequencies for all recordings (baseline, shock and recovery). Because recordings during exposure to an electrical field were affected by strong spatial drifts of the preparation and image registration and across-frames segmentation of ROIs were therefore not possible, PSD for each pixel in each recording for all fish was calculated, using the entire recording length of each raw image time series without any preprocessing. Calcium traces for all pixels were first detrended by subtracting the mean, then PSDs were calculated. Finally, the mean PSD spectrum of all pixels was calculated for all recordings. To prove that a large drift in the recording won't significantly affect the mean PSD spectrum, and that the most prominent frequencies will still be visible, a 100-pixel drift over 720 frames (6 min) was simulated for a stable baseline recording and PSD was calculated subsequently (supplementary Fig. 4). PSD results were analyzed via 2-way repeated measures ANOVA with Tukey's honest significant difference (HSD).

Declarations

Data availability statement

All data of this study is available from the corresponding author upon request.

Author Contributions

Conceptualization, A.B.A., D.S.B., F.A.D.; Methodology, D.S.B., A.B.A. C.L.; Setup Development, D.S.B., A.B.A., C.L.; Formal Analysis, D.S.B.; Investigation, D.S.B., C.L.; Resources, A.B.A.; Data Curation, D.S.B.; Writing, D.S.B., A.B.A, F.A.D, C.B..; Visualization, D.S.B., A.B.A., C.T.; Project Administration, A.B.A.; Funding Acquisition, A.B.A., D.S.B, F.A.D.

Competing Interests

The authors declare no competing interests.

References

1. Lidster, K., Readman, G. D., Prescott, M. J. & Owen, S. F. International survey on the use and welfare of zebrafish Danio rerio in research. *J. Fish Biol.* **90**, 1891–1905 (2017).
2. Tavares, B. & Lopes, S. S. The Importance of Zebrafish in Biomedical Research. *Acta Médica Port.* **26**, 583–592 (2013).
3. Lawrence, C. New frontiers for zebrafish management. in *Methods in Cell Biology* vol. 135 483–508 (Elsevier, 2016).
4. Russel, W. M. S. & Burch, R. L. *The Principles of Humane Experimental Technique*. (Methuen, 1959).
5. Clemence, M. & Leaman, J. Public attitudes to animal research in 2016. (2016).
6. Rose, J. D. *et al.* Can fish really feel pain? *Fish Fish.* **15**, 97–133 (2014).
7. Sneddon, L. U. Pain in aquatic animals. *J. Exp. Biol.* **218**, 967–976 (2015).
8. Collymore, C. Chapter 34 - Anesthesia, Analgesia, and Euthanasia of the Laboratory Zebrafish. *Zebrafish Biomed. Res.* 403–413 (2020) doi:10.1016/B978-0-12-812431-4.00034-8.
9. Valentim, A. M., van Eeden, F. J., Strähle, U. & Olsson, I. A. S. Euthanizing zebrafish legally in Europe. *EMBO Rep.* **17**, 1688–1689 (2016).
10. Strykowski, J. L. & Schech, J. M. Effectiveness of recommended euthanasia methods in larval zebrafish (Danio rerio). *J. Am. Assoc. Lab. Anim. Sci. JAALAS* **54**, 81–84 (2015).
11. Rombough, P. J. Ontogenetic changes in the toxicity and efficacy of the anaesthetic MS222 (tricaine methanesulfonate) in zebrafish (Danio rerio) larvae. *Comp. Biochem. Physiol. A. Mol. Integr. Physiol.* **148**, 463–469 (2007).

12. Readman, G. D., Owen, S. F., Murrell, J. C. & Knowles, T. G. Do Fish Perceive Anaesthetics as Aversive? *PLOS ONE* **8**, e73773 (2013).
13. Wilson, J. M., Bunte, R. M. & Carty, A. J. Evaluation of Rapid Cooling and Tricaine Methanesulfonate (MS222) as Methods of Euthanasia in Zebrafish (Danio rerio). *J. Am. Assoc. Lab. Anim. Sci.* **48**, 785–789 (2009).
14. Wong, D., Keyserlingk, M. A. G. von, Richards, J. G. & Weary, D. M. Conditioned Place Avoidance of Zebrafish (Danio rerio) to Three Chemicals Used for Euthanasia and Anaesthesia. *PLOS ONE* **9**, e88030 (2014).
15. Köhler, A. *et al.* Report of Workshop on Euthanasia for Zebrafish—A Matter of Welfare and Science. *Zebrafish* **14**, 547–551 (2017).
16. Wallace, C. K. *et al.* Effectiveness of Rapid Cooling as a Method of Euthanasia for Young Zebrafish (Danio rerio). *J. Am. Assoc. Lab. Anim. Sci.* **57**, 58–63 (2018).
17. Leyden, C. *et al.* Efficacy of Tricaine (MS-222) and Hypothermia as Anesthetic Agents for Blocking Sensorimotor Responses in Larval Zebrafish. *Front. Vet. Sci.* **9**, 864573 (2022).
18. Lines, J. A., Robb, D. H., Kestin, S. C., Crook, S. C. & Benson, T. Electric stunning: a humane slaughter method for trout. *Aquac. Eng.* **28**, 141–154 (2003).
19. Mocho, J.-P. *et al.* A Multi-Site Assessment of Anesthetic Overdose, Hypothermic Shock, and Electrical Stunning as Methods of Euthanasia for Zebrafish (Danio rerio) Embryos and Larvae. *Biology* **11**, 546 (2022).
20. Bohl, R. J., Henry, T. B. & Strange, R. J. Electroshock-induced mortality in freshwater fish embryos increases with embryo diameter: a model based on results from 10 species. *J. Fish Biol.* **76**, 975–986 (2010).
21. Bohl, R. J., Henry, T. B., Strange, R. J. & Rakes, P. L. Effects of Electroshock on Cyprinid Embryos: Implications for Threatened and Endangered Fishes. *Trans. Am. Fish. Soc.* **138**, 768–776 (2009).
22. Dwyer, W. P. & Erdahl, D. A. Effects of Electroshock Voltage, Wave Form, and Pulse Rate on Survival of Cutthroat Trout Eggs. *North Am. J. Fish. Manag.* **15**, 647–650 (1995).
23. Henry, T. B., Grizzle, J. M., Johnston, C. E. & Osborne, J. A. Susceptibility of Ten Fish Species to Electroshock-Induced Mortality. *Trans. Am. Fish. Soc.* **133**, 649–654 (2004).
24. Hollender, B. A. & Carline, R. F. Injury to Wild Brook Trout by Backpack Electrofishing. *North Am. J. Fish. Manag.* **14**, 643–649 (1994).
25. Reynolds, J.B. *Electrofishing*. (1996).
26. Teulier, L., Guillard, L., Leon, C., Romestaing, C. & Voituron, Y. Consequences of electroshock-induced narcosis in fish muscle: from mitochondria to swim performance. *J. Fish Biol.* **92**, 1805–1818 (2018).
27. Nusslein-Volhard, C. & Dahm, R. *Zebrafish*. (Oxford University Press, Oxford, New York, 2002).
28. Meyer, R. E. Euthanasia and Humane Killing. in *Veterinary Anesthesia and Analgesia* 130–143 (John Wiley & Sons, Ltd, 2015). doi:10.1002/9781119421375.ch6.

29. Parichy, D. M., Elizondo, M. R., Mills, M. G., Gordon, T. N. & Engeszer, R. E. Normal table of postembryonic zebrafish development: Staging by externally visible anatomy of the living fish. *Dev. Dyn.* **238**, 2975–3015 (2009).
30. Müller, U. K. & van Leeuwen, J. L. Swimming of larval zebrafish: ontogeny of body waves and implications for locomotory development. *J. Exp. Biol.* **207**, 853–868 (2004).
31. Vibert, R. Neurophysiology of Electric Fishing. *Trans. Am. Fish. Soc.* **92**, 265–275 (1963).
32. Muto, A., Ohkura, M., Abe, G., Nakai, J. & Kawakami, K. Real-Time Visualization of Neuronal Activity during Perception. *Curr. Biol.* **23**, 307–311 (2013).
33. Thompson, A. W., Vanwalleghem, G. C., Heap, L. A. & Scott, E. K. Functional Profiles of Visual-, Auditory-, and Water Flow-Responsive Neurons in the Zebrafish Tectum. *Curr. Biol.* **26**, 743–754 (2016).
34. Easter, Jr., Stephen S. & Nicola, G. N. The Development of Vision in the Zebrafish (Danio rerio). *Dev. Biol.* **180**, 646–663 (1996).
35. Niell, C. M. & Smith, S. J. Functional Imaging Reveals Rapid Development of Visual Response Properties in the Zebrafish Tectum. *Neuron* **45**, 941–951 (2005).
36. Nguyen, P. L., Yefimov, B. A., Coffin, A. & Cooper, C. Electroimmobilization as an Alternative Method to Chemical Immobilization of Larval Fish. *Trans. Am. Fish. Soc.* **148**, 725–738 (2019).
37. Lutnesky, M. M. F., Cradock, K. R. & Reynolds, J. B. Immobilization Threshold and Fish Conductivity of Two Small Fishes. *North Am. J. Fish. Manag.* **39**, 788–792 (2019).
38. AVMA Guidelines for the Euthanasia of Animals. https://olaw.nih.gov/policies-laws/avma-guidelines-2020.htm (2020).
39. Collymore, C., Banks, E. K. & Turner, P. V. Lidocaine Hydrochloride Compared with MS222 for the Euthanasia of Zebrafish (Danio rerio). *J. Am. Assoc. Lab. Anim. Sci.* **55**, 816–820 (2016).
40. Ferreira, J. M. *et al.* Anesthesia Overdose Versus Rapid Cooling for Euthanasia of Adult Zebrafish. *Zebrafish* **19**, 148–159 (2022).
41. Nordgreen, A. H., Slinde, E., Møller, D. & Roth, B. Effect of Various Electric Field Strengths and Current Durations on Stunning and Spinal Injuries of Atlantic Herring. *J. Aquat. Anim. Health* **20**, 110–115 (2008).
42. Robb, D. H. F., O' Callaghan, M., Lines, J. A. & Kestin, S. C. Electrical stunning of rainbow trout (Oncorhynchus mykiss): factors that affect stun duration. *Aquaculture* **205**, 359–371 (2002).
43. Snyder, D. E. *Electrofishing and Its Harmful Effects on Fish*. https://apps.dtic.mil/sti/pdfs/ADA420879.pdf (2003).
44. Dolan, C. R. & Miranda, L. E. Injury and Mortality of Warmwater Fishes Immobilized by Electrofishing. *North Am. J. Fish. Manag.* **24**, 118–127 (2004).
45. Sharber, N. G., Carothers, S. W., Sharber, J. P., De Vos, J. C. & House, D. A. Reducing Electrofishing-Induced Injury of Rainbow Trout. *North Am. J. Fish. Manag.* **14**, 340–346 (1994).

46. Henry, T. B. & Grizzle, J. M. Survival of largemouth bass, bluegill and channel catfish embryos after electroshocking. *J. Fish Biol.* **64**, 1206–1216 (2004).
47. Halloran, M. C. *et al.* Laser-induced gene expression in specific cells of transgenic zebrafish. *Development* **127**, 1953–1960 (2000).
48. Ádám, A., Bártfai, R., Lele, Z., Krone, P. H. & Orbán, L. Heat-Inducible Expression of a Reporter Gene Detected by Transient Assay in Zebrafish. *Exp. Cell Res.* **256**, 282–290 (2000).
49. Hardy, M. E., Ross, L. V. & Chien, C.-B. Focal gene misexpression in zebrafish embryos induced by local heat shock using a modified soldering iron. *Dev. Dyn.* **236**, 3071–3076 (2007).
50. Murtha, J. M. & Keller, E. T. Characterization of the heat shock response in mature zebrafish (*Danio rerio*). *Exp. Gerontol.* **38**, 683–691 (2003).
51. Cho, M. R., Thatte, H. S., Silvia, M. T. & Golan, D. E. Transmembrane calcium influx induced by ac electric fields. *FASEB J.* **13**, 677–683 (1999).
52. Duchen, M. R. Contributions of mitochondria to animal physiology: from homeostatic sensor to calcium signalling and cell death. *J. Physiol.* **516**, 1–17 (1999).
53. Garcia-Dorado, D., Ruiz-Meana, M., Inserte, J., Rodriguez-Sinovas, A. & Piper, H. M. Calcium-mediated cell death during myocardial reperfusion. *Cardiovasc. Res.* **94**, 168–180 (2012).
54. Hajnóczky, G., Davies, E. & Madesh, M. Calcium signaling and apoptosis. *Biochem. Biophys. Res. Commun.* **304**, 445–454 (2003).
55. Smaili, S. *et al.* Calcium and cell death signaling in neurodegeneration and aging. *An. Acad. Bras. Ciênc.* **81**, 467–475 (2009).
56. Batista Napotnik, T., Polajžer, T. & Miklavčič, D. Cell death due to electroporation – A review. *Bioelectrochemistry* **141**, 107871 (2021).
57. Xu, D. *et al.* General anesthetics protects against cardiac arrest-induced brain injury by inhibiting calcium wave propagation in zebrafish. *Mol. Brain* **10**, 44 (2017).
58. Spong, K. E., Andrew, R. D. & Robertson, R. M. Mechanisms of spreading depolarization in vertebrate and insect central nervous systems. *J. Neurophysiol.* **116**, 1117–1127 (2016).
59. Woitzik, J. *et al.* Propagation of cortical spreading depolarization in the human cortex after malignant stroke. *Neurology* **80**, 1095–1102 (2013).
60. Andreassen, A. H., Hall, P., Khatibzadeh, P., Jutfelt, F. & Kermen, F. Brain dysfunction during warming is linked to oxygen limitation in larval zebrafish. *Proc. Natl. Acad. Sci.* **119**, e2207052119 (2022).
61. Rijn, C. M. van., Krijnen, H., Menting-Hermeling, S. & Coenen, A. M. L. Decapitation in Rats: Latency to Unconsciousness and the 'Wave of Death'. *PLoS ONE* **6**, e16514 (2011).
62. Zandt, B.-J., Haken, B. ten, Dijk, J. G. van & Putten, M. J. A. M. van. Neural Dynamics during Anoxia and the "Wave of Death". *PLOS ONE* **6**, e22127 (2011).
63. Lambooij, E., Gerritzen, M. A., Reimert, H., Burggraaf, D. & van de Vis, J. W. A humane protocol for electro-stunning and killing of Nile tilapia in fresh water. *Aquaculture* **275**, 88–95 (2008).

64. Lambooij, E., Kloosterboer, R. J., Gerritzen, M. A. & van de Vis, J. W. Assessment of electrical stunning in fresh water of African Catfish (Clarias gariepinus) and chilling in ice water for loss of consciousness and sensibility. *Aquaculture* **254**, 388–395 (2006).
65. Würbel, H. More than 3Rs: the importance of scientific validity for harm-benefit analysis of animal research. *Lab Anim.* **46**, 164–166 (2017).
66. Sneddon, L. U. Clinical Anesthesia and Analgesia in Fish. *J. Exot. Pet Med.* **21**, 32–43 (2012).
67. Schindelin, J. *et al.* Fiji: an open-source platform for biological-image analysis. *Nat. Methods* **9**, 676–682 (2012).
68. Walker, P., Lerski, R. A., Mathur-De Vré, R., Binet, J. & Yane, F. VI. Preparation of agarose gels as reference substances for NMR relaxation time measurement. *Magn. Reson. Imaging* **6**, 215–222 (1988).
69. Pachitariu, M. *et al.* Suite2p: beyond 10,000 neurons with standard two-photon microscopy. 061507 Preprint at https://doi.org/10.1101/061507 (2017).
70. Miri, A., Daie, K., Burdine, R. D., Aksay, E. & Tank, D. W. Regression-Based Identification of Behavior-Encoding Neurons During Large-Scale Optical Imaging of Neural Activity at Cellular Resolution. *J. Neurophysiol.* **105**, 964–980 (2011).

Figures

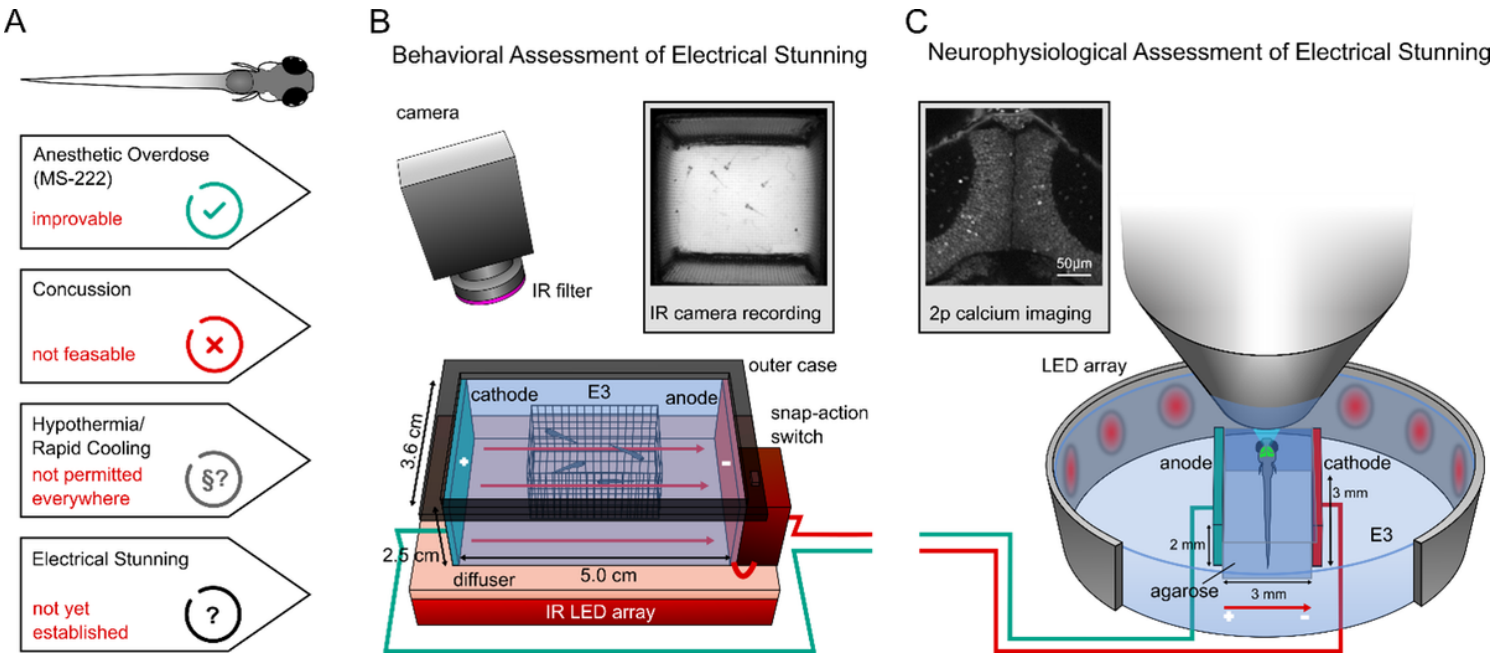

Figure 1

Developing a protocol for humane euthanasia via electrical stunning. **(A)** Illustration of approved euthanasia methods for zebrafish. **(B)** The Electrical stunning chamber with cuboid net container allows imaging of behavior. **(C)** The brain activity of immobilized animals can be measured during visual stimulation and electrical stunning.

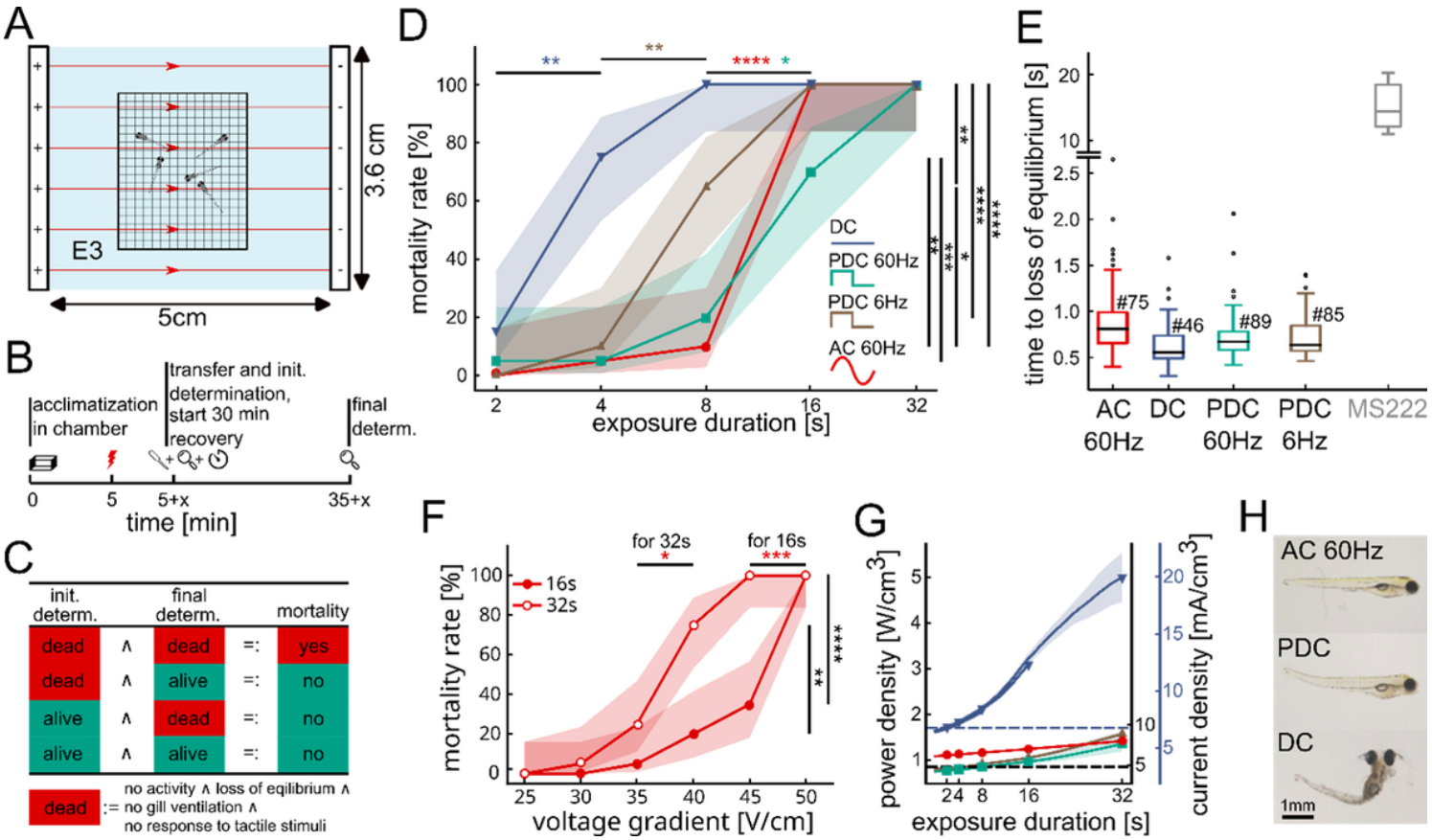

Figure 2

Electric AC fields are well-suited for euthanasia of larvae. **(A)** Schematic of the experimental setup. **(B)** Protocol for assessing mortality. **(C)** Logical matrix defining under which condition within the experimental procedure, a larva was considered dead. **(D)** Mortality rates of different voltage types for different exposure durations at a voltage gradient of 50 V/cm. Asterisks indicate significances by z-test for proportions followed by Bonferroni correction between exposure durations (colored asterisks) and voltage types (black asterisks). Envelopes show 95 % Wilson confidence intervals. **(E)** Time to loss of equilibrium for different voltage types (animal numbers are provided next to the # sign) For comparison, the time to loss of equilibrium for MS-222 (336 mg/l) is shown in gray [17]. **(F)** Mortality rates of 16 s and 32 s exposure duration for different voltage gradients at AC voltage. Asterisks indicate significance by z-test for proportions followed by Bonferroni correction between voltage gradients and exposure durations. Envelopes show 95 % Wilson confidence intervals. **(G)** Power density and current density of different voltage types for different exposure durations at 50 V/cm. Power and current densities were calculated based on measured currents during the experiment. Dashed lines indicate the expected power density without joule heating (dark blue: DC, black: AC and PDC). Envelopes show standard deviation. **(H)** Morphological effects of electrical stunning at 50 V/cm, 32 s, directly after exposure.

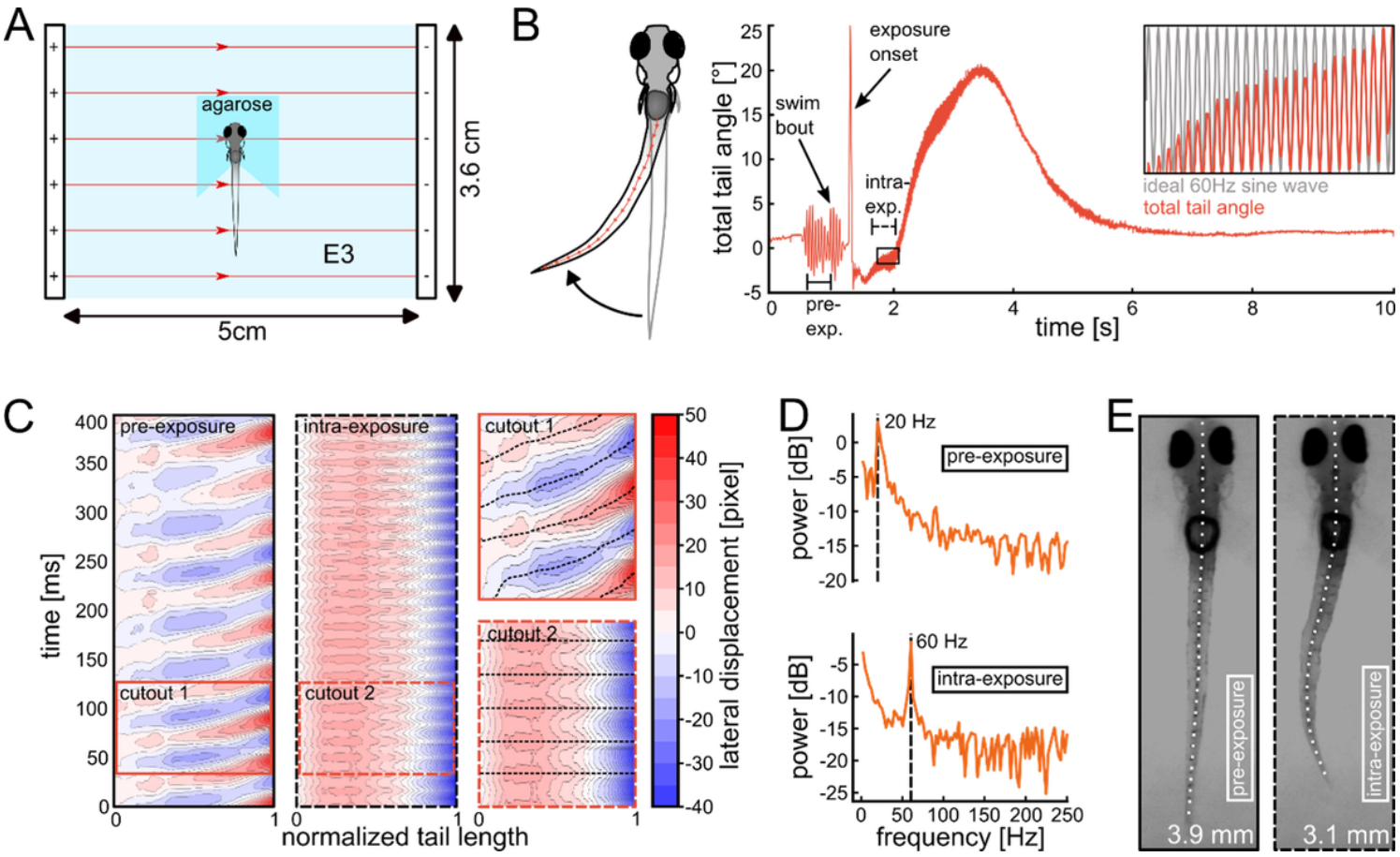

Figure 3

The AC field drives direct muscle contractions. **(A)** Schematic of the experimental setup, agarose surrounding the larva's tail has been removed. **(B)** Left: schematic of larva illustrating tail displacement during electrical stunning. Orange arrows indicate skeleton used for computing total tail angle. Right: Total tail angle during exposure. Arrows indicate a spontaneous swim bout and the exposure onset. Inset shows the tail angle during exposure, which perfectly matched a 60 Hz sinusoidal wave. **(C)**Lateral tail displacement profile before (left, pre-exposure) and during (right, intra-exposure) electrical stunning. Time periods of the profiles are indicated in (B) as straight and dashed bars. Dashed lines in cutouts indicate position of extremes in time and space. **(D)** Power spectrum of pre-exposure (top) and intra-exposure (bottom) periods. **(E)** Length of the larva before (left) and during (right) electrical stunning.

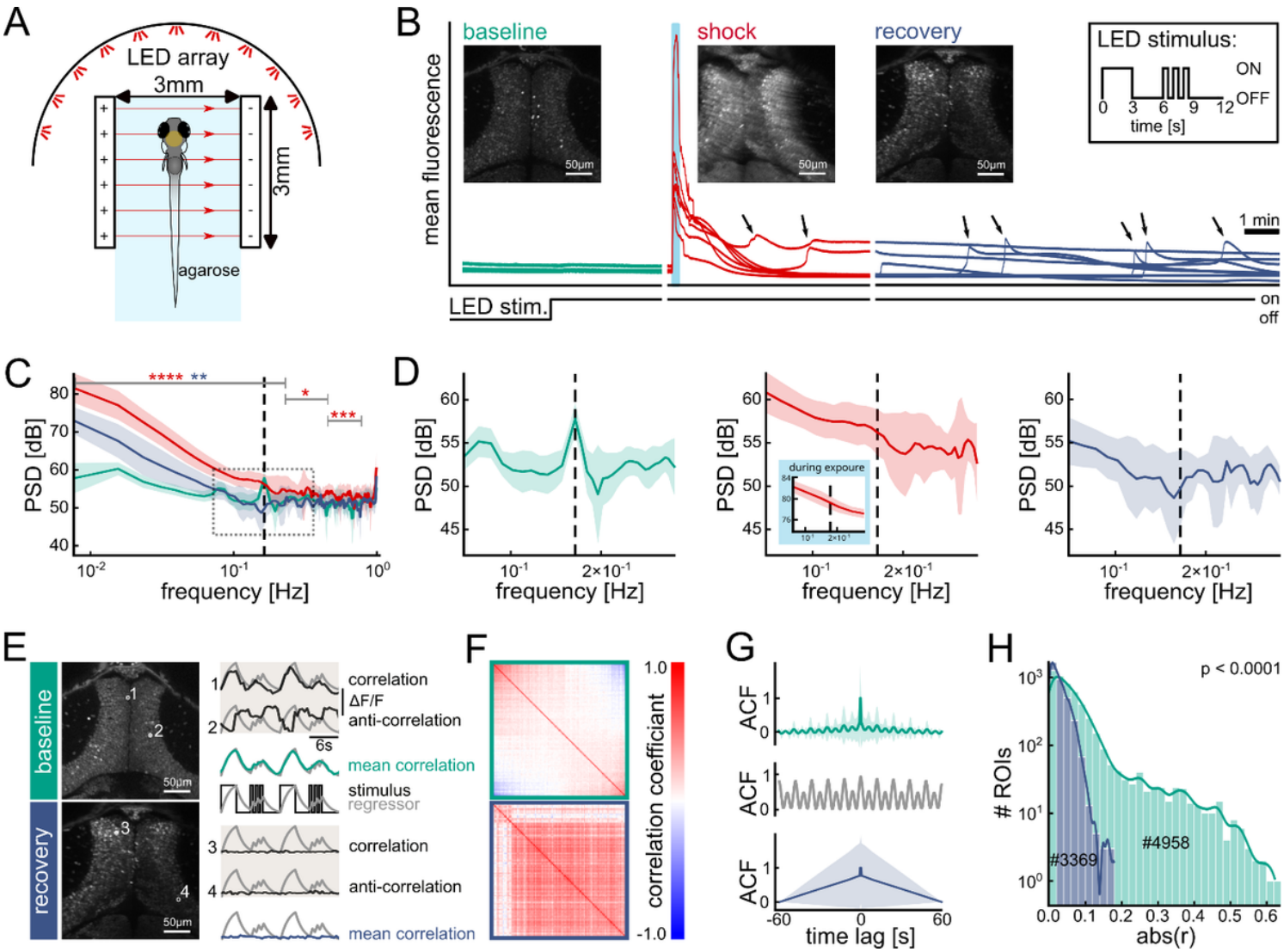

Figure 4

Absence of sensory-evoked neural activity during and after electrical stunning. **(A)** Schematic of experimental setup positioned under the two-photon microscope. Yellow dot indicates the imaged brain area (optic tectum). **(B)** Mean calcium signals for baseline, shock and recovery recording for all fish (one trace per fish). Light blue bar indicates exposure duration. LED stimulus trace indicates when visual stimulus was used or not. Arrows highlight occurrence of slowly propagating calcium waves occurring after electrical stunning. **(C)** Power spectral density (PSD) for baseline, shock and recovery recording (green, red and dark blue as used in (B)). Envelopes show standard deviation. Dashed line indicates the visual stimulus main frequency of 0.1667 Hz. Asterisks indicate periods with significant differences to baseline recording (two-way repeated measures ANOVA followed by Tukey's HSD test). **(D)** Inset of (C) for baseline, shock and recovery recording. **(E)**Example calcium traces of neurons (black) (anti-) correlated with the stimulus (gray), and mean correlation traces (green and dark blue) of 20% best correlated ROIs for baseline and recovery recording. **(F)** ROI cross-correlation matrices for baseline and recovery recording (top and bottom). **(G)**Auto-correlation function (ACF) for baseline and recovery recording (top and bottom). Envelopes show standard deviation. Grey shows ACF for the stimulus (regressor) itself. **(H)**

Histogram of absolute ROI cross-correlation coefficients for baseline and recovery recordings. P-value derived from Levene-test.

Supplementary Files

This is a list of supplementary files associated with this preprint. Click to download.

- supplemetarymaterial.docx
- supplvideo1.avi
- supplvideo2.avi
- supplvideo3.avi